Inorganic Chemistry

Article

pubs.acs.org/IC

Oxyanion-Encapsulated Caged Supramolecular Frameworks of a Tris(urea) Receptor: Evidence of Hydroxide- and Fluoride-Ion-Induced Fixation of Atmospheric CO_2 as a Trapped CO_3^{2-} Anion

Sandeep Kumar Dey, Romen Chutia, and Gopal Das*

Department of Chemistry, Indian Institute of Technology Guwahati, Assam 781039, India

Supporting Information

ABSTRACT: A tris(2-aminoethyl)amine-based tris(urea) receptor, **L**, with electron-withdrawing *m*-nitrophenyl terminals has been established as a potential system that can efficiently capture and fix atmospheric CO_2 as air-stable crystals of a CO_3^{2-}-encapsulated molecular capsule (complex **1**), triggered by the presence of *n*-tetrabutylammonium hydroxide/fluoride in a dimethyl sulfoxide solution of **L**. Additionally, **L** in the presence of excess HSO_4^- has been found to encapsulate a divalent sulfate anion (SO_4^{2-}) within a dimeric capsular assembly of the receptor (complex **2**) via hydrogen-bonding-activated proton transfer between the free and bound HSO_4^- anions. Crystallographic results show proof of oxyanion encapsulation within the centrosymmetric cage of **L** via multiple N−H···O hydrogen bonds to the six urea functions of two inversion-symmetric molecules. The solution-state binding and encapsulation of oxyanions by N−H···O hydrogen bonding has also been confirmed by quantitative ^{1}H NMR titration experiments, 2D NOESY NMR experiments, and Fourier transform IR analyses of the isolated crystals of the complexes that show huge spectral changes relative to the free receptor.

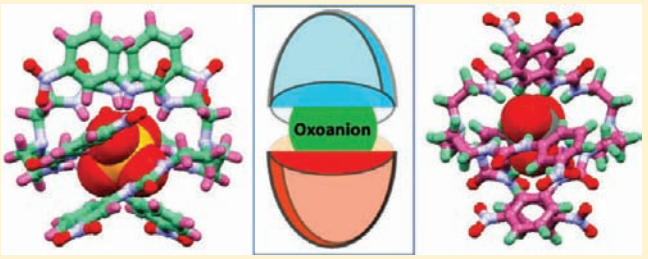

1. INTRODUCTION

The field of anion receptor chemistry continues to expand its horizon with new synthetic hosts capable of recognizing anions with environmental and biomedical relevance.[1] The observations in natural systems have inspired researchers to develop numerous neutral receptors that employ hydrogen bonds offered by specific binding sites from amide,[2] urea,[3] pyrrole,[4] and indole[5] functionalities for the recognition and binding of anionic guests on suitable frameworks. Acyclic podand receptors with multiarmed hydrogen-bonding functionality have been shown to coordinate with targeted anionic species via the formation of capsular assemblies.[6] One of the most fascinating features of molecular capsules is their ability to create a distinct microenvironment that isolates the encapsulated guest from the bulk of the solvent media and thereby leads to phenomena such as molecular sorting when the possible formation of different capsules is present in the same solution.[7] When two receptor molecules with interior anion-binding elements create a dimeric capsular assembly, there is a possibility to satisfy the higher coordination numbers required for the binding of oxyanions and hydrated anions. Anions generally have very high solvation energies that must be compensated for by the host for effective anion recognition.[8] Thus, it is the design of sophisticated three-dimensional architectures that is essential to fully encapsulate the anions by creating a highly specific anion-binding pocket/cavity. Urea-functionalized tripodal scaffolds offer a flexible and structurally preorganized cavity, which has been widely employed in the binding and recognition of anions because of their favorable conformation for multiple hydrogen bonds that favors the formation of a stable host/guest complex.[9] Although numerous synthetic molecular capsules have been achieved to date, the challenges still exist to control the capsular assembly formation in the presence of a guest anion that acts as a template in the process. Template-induced association of molecular species represents one of the main approaches in the control of caged supramolecular assembly formation.

Among several oxyanions, the deleterious effect of sulfate has been recognized as a major hurdle to cleanup efforts in the remediation of nuclear waste; e.g., contamination of the Hanford nuclear waste site (USA) by this anion has been a matter of increased concern, hampering the vitrification process.[10] Because of its large standard Gibbs energy of hydration (−1080 kJ mol^{-1}), extraction of sulfate ions from an aqueous to an organic phase presents a particularly challenging task.[10b] Nature responds to this challenge by encapsulating the sulfate anion with an array of seven hydrogen bonds, as observed in the sulfate-binding protein (SBP) of *Salmonella typhimurium*, which was structurally identified in 1985 by Pflugrath and Quiocho.[11] The crystal structure of SBP reveals that an individual sulfate anion is completely encapsulated within the core of the protein (7 Å below the surface), between the two lobes of SBP through seven hydrogen bonds including five peptide −NH groups, one serine −OH group, and one tryptophan −NH group. In recent years, some receptors purely

Received: September 19, 2011
Published: January 10, 2012

dx.doi.org/10.1021/ic2020379 | *Inorg. Chem.* 2012, 51, 1727−1738

based on organic frameworks have been shown to encapsulate the sulfate anion in a 1:1 or 2:1 (host/guest) ratio, and a couple of them have been efficiently employed in sulfate-ion separation based on liquid/liquid anion-exchange technology or competitive crystallization techniques.[9a,e] Thus, for effective binding and encapsulation of anions in nature, the receptor framework should be designed with a complementary cavity surrounded by optimally arranged binding sites, which eventually induce high chelate effects by coordinating with the targeted anionic species.

Another major environmental issue of utmost concern is the significant rise in the CO_2 concentration in the atmosphere caused by increased consumption of fossil fuels and the overgrowing number of industries, automobiles, etc., which eventually demands the efficient fixation and activation of atmospheric CO_2 into green chemicals.[12] Microporous aluminosilicates, silica gel, activated carbons, and metal−organic frameworks (MOFs) have widely been employed to capture and store CO_2 among other approaches, which utilize the effective conversion of CO_2 into green chemicals for the synthesis of specific chemical intermediates.[13] However, in light of supramolecular chemistry, efficient fixation of aerial CO_2 as carbonate/bicarbonate can been achieved with artificial hydrogen-bonding receptors in the presence of hydroxide and fluoride ions.[14] Furthermore, Gale et al. have also demonstrated CO_2 capture as carbamates (alkylammonium/alkylcarbamate) by a series of urea-based receptors in the presence of aliphatic amines (CO_2 scrubbers) bubbled with CO_2 in dimethyl sulfoxide (DMSO).[15]

Given our interest in the field of anion receptor chemistry,[16] herein, we report both hydroxide- and fluoride-ion-induced efficient fixation of atmospheric CO_2 as air-stable crystals of a carbonate-entrapped hydrogen-bonding capsule of a nitro-functionalized tris(urea) receptor, **L** (Scheme 1), in DMSO

Scheme 1. Molecular Structure of a Tris(urea) Receptor, L

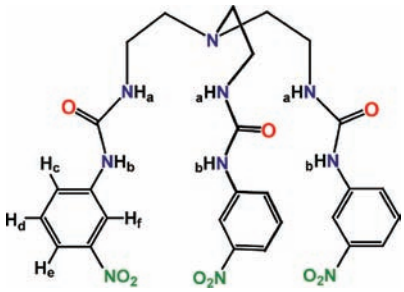

along with detailed solution-state binding studies. Furthermore, we also account for the structural evidence of an optimally coordinated divalent sulfate anion encapsulated within a dimeric capsular assembly of the receptor (**L**) by 12 N−H···O hydrogen bonds.

2. EXPERIMENTAL SECTION

2.1. Materials and Methods. All reagents and solvents were obtained from commercial sources and used as received without further purification. Tris(2-aminoethyl)amine (tren), 3-nitrophenyl isocyanate, and tetraalkylammonium salts were purchased from Sigma-Aldrich and used as received. Solvents for synthesis and crystallization experiments were purchased from Merck, India, and used as received. ^{1}H NMR spectra were recorded on a Varian FT-400 MHz instrument, and chemical shifts were recorded in parts per million (ppm) on the scale using tetramethylsilane [$Si(CH_3)_4$] or a residual solvent peak as a reference, and ^{13}C spectra were obtained at 100 MHz. The electrospray ionization mass spectrometry (ESI-MS) spectrum of **L** was recorded in a Waters Q-Tof Premier liquid chromatography (LC)−MS system in methanol. The FT-IR spectra of air-dried samples were recorded on a Perkin-Elmer-Spectrum One FT-IR spectrometer with KBr disks in the range 4000−450 cm^{-1}. Thermal analysis was performed by using an SDTA 851-e TGA thermal analyzer (Mettler Toledo) with a heating rate of 5 °C min^{-1} in a N_2 atmosphere. X-ray diffraction (XRD) patterns of dried crystalline powder were recorded using a Bruker-D8 Advance X-ray diffractometer with Cu Kα radiation at λ = 0.154 18 nm. Crystals of complexes **1** and **2** were washed with a minimum amount of acetonitrile, followed by diethyl ether, and dried at room temperature by pressing between filter papers before thermogravimetric analysis (TGA).

Binding constants were obtained by ^{1}H NMR (Varian 400 MHz) titrations of **L** with tetraethylammonium (TEA)/*n*-tetrabutylammonium (*n*-TBA) salts of respective anions in DMSO-d_6 at 298 K. The initial concentration of the corresponding receptor solution was 5 mM. Aliquots of anions were added from 50 mM stock solutions of anions (up to 1:10 host/guest stoichiometry). The residual solvent peak in DMSO-d_6 (2.500 ppm) was used as an internal reference, and each titration was performed with 18−20 measurements at room temperature.

The following equation was used to determine the association constant (K) values:[17]

$$\Delta\delta = \{([A]_0 + [\mathbf{L}]_0 + 1/K) \pm [([A]_0 + [\mathbf{L}]_0 + 1/K)^2 - 4[\mathbf{L}]_0[A]_0]^{1/2}\}\Delta\delta_{max}/2[\mathbf{L}]_0$$

where **L** = ligand and A = anion. An error limit in K was less that 10%.

2.2. Synthesis and Characterization of L. Tripodal receptor **L** was synthesized by modification of a reported literature procedure[9b] where the reaction of tris(2-aminoethyl)amine (tren) with 3-nitrophenyl isocyanate in a 1:3 molar ratio at room temperature yielded **L** in quantitative yield. A total of 2.460 g (15 mmol) of 3-nitrophenyl isocyanate was dissolved in 30 mL of dry tetrahydrofuran (THF) in a 100 mL round-bottomed flask and 0.730 mL (5 mmol) of tren dissolved in 10 mL of dry THF were added dropwise (using a dropping funnel) over a period of 1 h with constant stirring at room temperature. The resulting solution mixture was stirred overnight at room temperature when a pale-yellow precipitate was observed to be formed. Then, the volume of the solvent (THF) was reduced to around 10 mL in vacuo, and the obtained solid product was filtered off and washed with 10 mL of dichloromethane a couple of times to remove the unreacted reagents. The pale-yellow precipitate thus collected was dried in air and characterized by NMR, FT-IR, ESI-MS, and single-crystal XRD analyses. Yield of **L**: 84%. ^{1}H NMR (DMSO-d_6, 400 MHz): δ (ppm) 2.64 (d, 6H, $-NCH_2$), 3.23 (d, 6H, $-NCH_2CH_2$), 6.31 (s, 3H, urea −NHa), 7.41 (t, 3H, ArCH), 7.59 (d, 3H, ArCH), 7.66 (d, 3H, ArCH), 8.44 (s, 3H, ArCH), 9.07 (s, 3H, urea $-NH_b$). ^{13}C NMR (100 MHz, DMSO-d_6): δ (ppm) 37.72 (×3C, $-NCH_2$), 53.78 (×3C, $-NCH_2CH_2$), 111.58 (×3C, ArH), 115.40 (×3C, ArH), 123.62 (×3C, ArH), 129.77 (×3C, ArH), 141.83 (×3C, ArH), 148.08 (×3C, ArH), 155.08 (×3C, C═O). FT-IR (ν, cm^{-1}): 1245 (C−N), 1350 (NO_2 sym), 1527 (NO_2 asym), 1597 (C═C), 1655 (−C═O), 3328 (N−H). ESI-MS, $[M + 1]^+$ m/z = 639.2498.

Synthesis and Characterization of Complex 2TBA[2L·(CO_3^{2-})] (1). Carbonate-encapsulated complex **1** was initially obtained by charging an excess (10 equiv) of *n*-tetrabutylammonium fluoride into a 5 mL DMSO solution of **L** (65 mg, 0.1 mmol). After the addition of F^- ions, the solution was stirred for about 15 min at room temperature and filtered in a test tube for crystallization. Slow evaporation of the filtrate at room temperature yielded colorless crystals suitable for single-crystal X-ray crystallographic analysis within 8−10 days. The isolated yield of **1** is 74% after 10 days.

Complex **1** can also be obtained in a comparatively much higher yield simply by adding an equimolar quantity of (*n*-TBA)OH to a 5 mL DMSO solution of **L**, which upon slow evaporation at room

dx.doi.org/10.1021/ic2020379 | Inorg. Chem. 2012, 51, 1727−1738

tempearture yielded air-stable crystals of **1** within 1 or 2 days. The isolated yield of **1** is 92% after 3 days. Mp: 185 °C. ^{1}H NMR (DMSO-d_6, 400 MHz): δ (ppm) 0.86 (t, 24H, TBA $-CH_3$), 1.25 (d, 16H, TBA $-CH_2$), 1.51 (s, 16H, TBA $-CH_2$), 2.52 (s, 12H, $-NCH_2$), 3.11 (s, 16H, TBA $-N^+CH_2$), 3.19 (s, 12H, $-NCH_2CH_2$), 7.18 (s, 6H, ArCH), 7.49 (d, 6H, ArCH), 7.59 (d, 6H, ArCH), 8.27 (s, 6H, ArCH), 10.50 (s, 6H, urea $-NH_b$). ^{13}C NMR (100 MHz, DMSO-d_6): δ (ppm) 13.43 (×8C, TBA $-CH_3$), 19.22 (×8C, TBA $-CH_2$), 23.08 (×8C, TBA $-CH_2$), 36.75 (×6C, $-NCH_2$), 53.41 (×6C, $-NCH_2CH_2$), 57.59 (×8C, TBA $-N^+CH_2$), 111.25 (×6C, ArH), 114.75 (×6C, ArH), 123.33 (×6C, ArH), 129.05 (×6C, ArH), 142.16 (×6C, ArH), 147.59 (×6C, ArH), 155.13 (×6C, −C═O), 171.98 (CO_3^{2-}). FT-IR (ν, cm^{-1}): 885 (CO_3^{2-}), 1238 (C−N), 1343 (NO_2 sym), 1523 (NO_2 asym), 1606 (C═C), 1699 (−C═O), 3390 (N−H).

Synthesis and Characterization of Complex 2TBA[2L·(SO_4^{2-})] (2). Sulfate-encapsulated complex **2** was obtained by adding an excess (10 equiv) of *n*-tetrabutylammonium hydrogensulfate into a 5 mL DMSO solution of **L** (65 mg, 0.1 mmol). After the addition of bisulfate ions, the solution was stirred for about 30 min at 60 °C and filtered in a test tube for crystallization. Slow evaporation of the filtrate at room temperature yielded colorless crystals suitable for single-crystal X-ray crystallographic analysis within 15 days of exposure to an unmodified atmosphere. The isolated yield of **2** is 58% after 15 days. Mp: 242 °C. ^{1}H NMR (DMSO-d_6, 400 MHz): δ (ppm) 0.88 (t, 24H, TBA $-CH_3$), 1.26 (q, 16H, TBA $-CH_2$), 1.52 (s, 16H, TBA $-CH_2$), 2.49 (s, 12H, $-NCH_2$), 3.12 (t, 16H, TBA $-N^+CH_2$), 3.21 (s, 12H, $-NCH_2CH_2$), 7.10 (t, 6H, ArCH), 7.33 (s, 6H, urea −NHa), 7.44 (d, 6H, ArCH), 7.57 (d, 6H, ArCH), 8.24 (s, 6H, ArCH), 9.58 (s, 6H, urea $-NH_b$). ^{13}C NMR (100 MHz, DMSO-d_6): δ (ppm) 13.50 (×8C, TBA $-CH_3$), 19.25 (×8C, TBA $-CH_2$), 23.10 (×8C, TBA $-CH_2$), 37.08 (×6C, $-NCH_2$), 54.34 (×6C, $-NCH_2CH_2$), 57.59 (×8C, TBA $-N^+CH_2$), 111.39 (×6C, ArH), 114.82 (×6C, ArH), 123.35 (×6C, ArH), 128.93 (×6C, ArH), 141.99 (×6C, ArH), 147.65 (×6C, ArH), 154.92 (×6C, −C═O). FT-IR (ν, cm^{-1}): 1089 (SO_4^{2-}), 1232 (C−N), 1351 (NO_2 sym), 1524 (NO_2 asym), 1600 (C═C), 1695 (−C═O), 3340 (N−H).

2.3. X-ray Crystallography. In each case, a crystal of suitable size was selected from the mother liquor and immersed in silicone oil, and it was mounted on the tip of a glass fiber and cemented using epoxy resin. The intensity data were collected using a Bruker SMART APEX-II CCD diffractometer, equipped with a fine-focus 1.75 kW sealed-tube Mo K_α radiation (λ = 0.710 73 Å) at 298(3) K, with increasing ω (width of 0.3° frame^{-1}) at a scan speed of 5 s frame^{-1}. *SMART* software was used for data acquisition. Data integration and reduction were undertaken with *SAINT* and *XPREP*[18] software. Multiscan empirical absorption corrections were applied to the data using the program *SADABS*.[19] Structures were solved by direct methods using *SHELXS-97*[20] and refined with full-matrix least squares on F^2 using *SHELXL-97*.[21] All non-hydrogen atoms were refined anisotropically, hydrogen atoms attached to all carbon atoms were geometrically fixed, and the positional and temperature factors are refined isotropically. Hydrogen atoms attached with the urea nitrogen atoms were located by an electron Fourier map and refined isotropically. Usually, temperature factors of hydrogen atoms attached to carbon atoms are refined by restraints −1.2 or −1.5 U_{iso}(C), although the isotropic free refinement is also acceptable. Structural illustrations have been drawn with *Mercury 2.3*[22] for Windows. Parameters for data collection and crystallographic refinement details of receptor **L** and complexes **1** and **2** are summarized in Table 1.

Table 1. Crystallographic Parameters and Refinement Details of L and Complexes 1 and 2

parameters	L	1	2
empirical formula	$C_{27}H_{30}N_{10}O_9$	$C_{87}H_{132}N_{22}O_{21}$	$C_{86}H_{132}N_{22}O_{22}S$
CCDC	833790	833791	833792
fw	638.61	1822.15	1858.21
cryst syst	triclinic	monoclinic	monoclinic
space group	$P\bar{1}$	$C2/c$	$C2/c$
a/Å	13.0495(4)	33.4669(13)	22.9827(10)
b/Å	13.4255(4)	15.1439(5)	13.3103(6)
c/Å	19.0544(9)	22.8357(10)	33.5349(15)
α/deg	99.512(2)	90.00	90.00
β/deg	98.195(2)	120.928(3)	98.705(2)
γ/deg	109.665(1)	90.00	90.00
V/Å^3	3029.0(2)	9928.0(7)	10140.4(8)
Z	4	4	4
D_c/g cm^{-3}	1.400	1.219	1.217
μ(Mo K_α)/mm^{-1}	0.108	0.088	0.108
T/K	298(2)	298(2)	298(2)
θ_{max}	27.860	21.630	19.600
total no. of reflns	37 783	48 123	41 939
indep reflns	11 778	5776	4384
obsd reflns	10 284	4045	3646
param refined	830	592	595
R1 [$I > 2\sigma(I)$]	0.0461	0.0496	0.0486
wR2 (all data)	0.1691	0.1831	0.1467
GOF (F^2)	0.964	1.030	0.983

3. RESULTS AND DISCUSSION

For a receptor to bind with the anionic guests, it should, in principle, possess preorganized anion-binding elements decorated on a suitable platform/framework. Receptor **L** possesses a highly organized tripodal scaffold with hydrogen-bonding urea functions suitable for anion binding and encapsulation. In addition, functionalization of **L** with π-acidic nitrophenyl moieties as aryl terminals significantly enhances the binding ability of the receptor toward anionic guest encapsulation. The chelate effect may also play an important role in the anion-binding affinity because of the favorable contributions from both entropy and enthalpy. Efforts were made to examine the solid-state binding of different anions with receptor **L**, by charging an excess *n*-TBA/TEA salt of anions to a solution of **L** in aprotic solvents like DMSO and MeCN. However, we were able to isolate only two complexes (**1** and **2**), as single crystals suitable for X-ray crystallographic analysis from individual solutions of **L** in the presence of anions such as fluoride and hydrogensulfate under identical crystallization conditions. It is important to mention here that crystals have proven to be difficult to obtain in the presence of other anions such as ClO_4^-, AcO^-, NO_3^-, and $H_2PO_4^-$, where we observed the formation of a thick oily liquid settling at the bottom of the crystallization vial in all cases. From the perspective of anion receptor chemistry, crystallization has traditionally been a route to understand the structural insights of the anion complexes formed, primarily by single-crystal XRD analysis, which are then related to the observed selectivity in solution. It is interesting to note that the quantitative yield of CO_3^{2-}-encapsulated complex **1** has been chiefly obtained from the receptor/F^- solution, where the source of CO_3^{2-} is from the atmospheric CO_2 that has been efficiently fixed by the in situ generated OH^- ions, whereas SO_4^{2-}-encapsulated complex **2** was primarily obtained from the receptor/HSO_4^- solution, where deprotonation of HSO_4^- can be attributed to hydrogen-bonding-activated proton transfer between the free and bound anions. Structural information obtained from XRD analysis of the carbonate and sulfate complexes (**1** and **2**) provides insight into the proper binding topology of the entrapped oxyanions with the neutral receptor molecule and anion-induced capsular assembly formation. Structural elucidation of complexes **1** and **2** revealed that coordination of oxyanions is primarily governed

dx.doi.org/10.1021/ic2020379 | *Inorg. Chem.* 2012, 51, 1727−1738

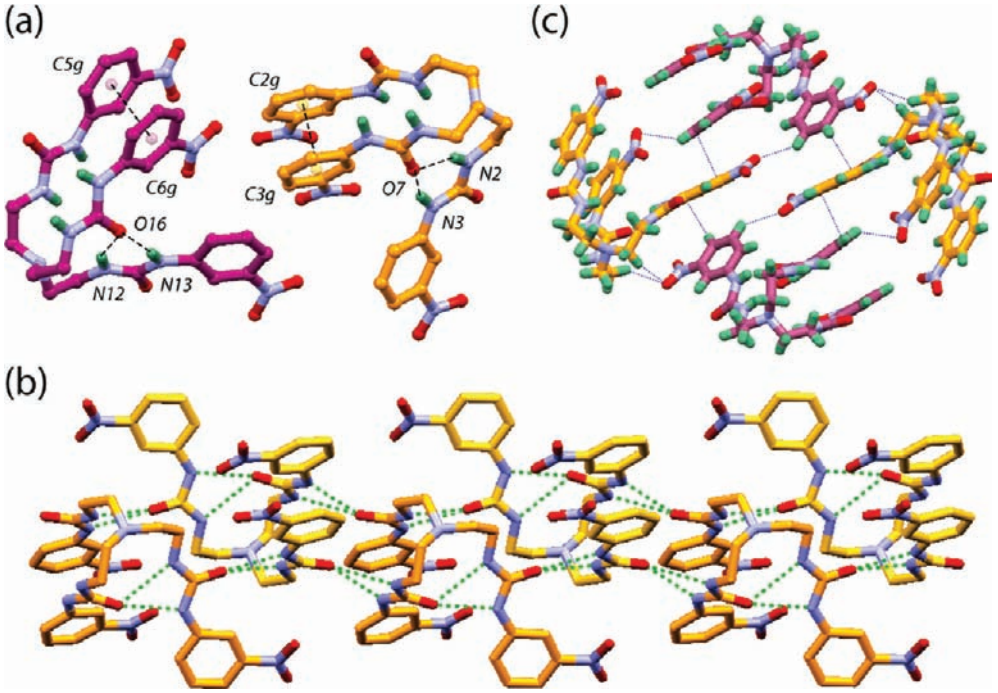

Figure 1. (a) X-ray structure of **L** (ball and stick) depicting the intramolecular N−H···O(carbonyl) hydrogen bonding and $\pi\cdots\pi$ stacking between the receptor side arms of individual symmetry-independent molecules (shown in different colors). (b) Complementary hydrogen bonding of the urea moieties forming a 1D bilayer network among molecules of identical symmetry in **L**. (c) Intermolecular C−H···O(nitro) and C−H···π interactions formed between the symmetry-independent molecules in **L**.

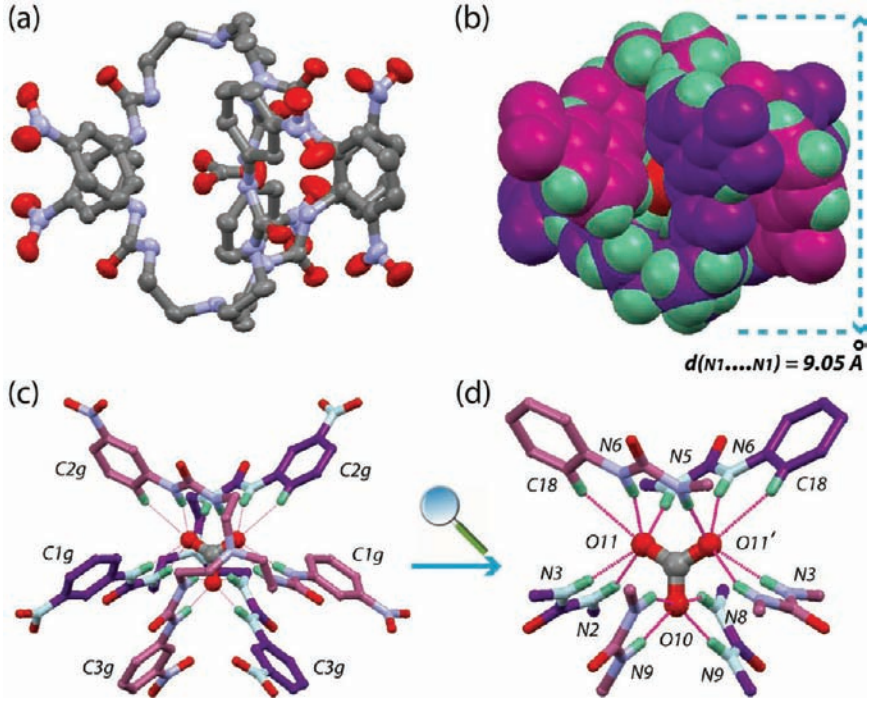

Figure 2. (a) Thermal ellipsoid plot (30% probability) of complex **1** depicting encapsulation of the CO_3^{2-} anion within the centrosymmetric cage of two inversion-symmetric molecules of **L**. (b) Spacefill representation depicting full encapsulation of the CO_3^{2-} anion. (c) Ball-and-stick representation depicting the 14 hydrogen-bonding contacts on CO_3^{2-} within the dimeric capsule of **L**. (d) Magnified view showing coordination of CO_3^{2-} with the 12 −NH groups and 2 aryl −CH protons of the dimeric capsule. TBA countercations are omitted for clarity of the presentation.

by multiple N−H···O(anion) interactions within the caged supramolecular assembly of two inversion-symmetric molecules of **L**. In addition, the complexes are further stabilized by various intermolecular C−H···O hydrogen bonds, which induce added rigidity to the anion-encapsulated molecular capsules and serve as the foundation for efficient crystallization of the desired complexes.

3.1. Structural Description of Receptor L. Single crystals of **L** suitable for XRD analysis were obtained from DMSO, which crystallizes in triclinic space group $P\bar{1}$ with $Z = 4$. The

dx.doi.org/10.1021/ic2020379 | *Inorg. Chem.* 2012, 51, 1727−1738

Table 2. Hydrogen-Bonding Contacts on CO_3^{2-} and SO_4^{2-} Anions within the Centrosymmetric Cage of L in Complexes 1 and 2

complex	D−H···O	d(H···O)/Å	d(D···O)/Å	∠D−H···O/deg
1	N2−H···O11	2.38(2)	3.151(4)	148(2)
	N3−H···O11	2.07(2)	2.912(4)	164(2)
	N5−H···O11	2.06(2)	2.926(3)	177(2)
	N6−H···O11	1.99(2)	2.831(3)	164(2)
	N9−H···O10	1.92(2)	2.781(3)	172(2)
	N8−H···O10	2.64(3)	3.358(2)	141(2)
	C18−H···O11	2.60(2)	3.344(4)	137(2)
2	N5−H···O10	2.17(4)	3.022(5)	168(2)
	N8−H···O10	2.25(4)	3.049(5)	153(3)
	N9−H···O10	2.15(4)	2.974(5)	159(2)
	N3−H···O11	2.02(3)	2.882(4)	172(2)
	N6−H···O11	1.99(3)	2.849(4)	174(2)
	N2−H···O11	2.69(3)	3.464(5)	150(3)

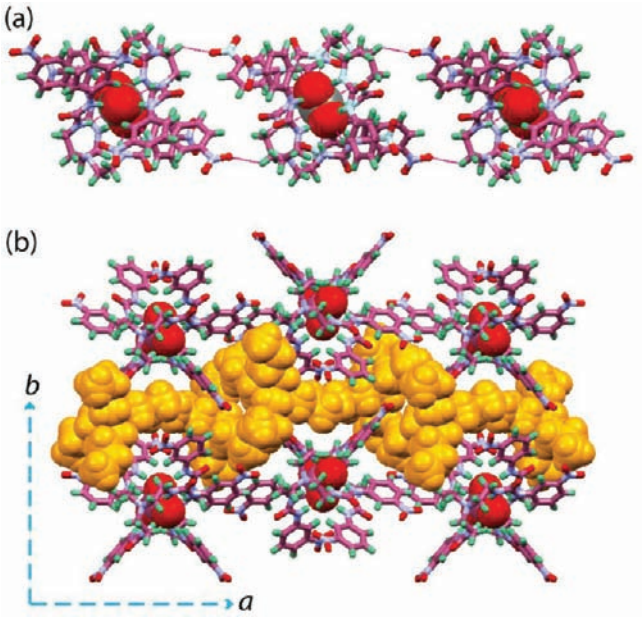

Figure 3. (a) Intermolecular C−H···O(nitro) hydrogen-bonded 1D chain of a carbonate-encapsulated molecular capsule along the crystallographic *a* axis. (b) Crystal packing in complex **1**, as viewed down the crystallographic *c* axis.

asymmetric unit contains two symmetry-independent receptor molecules (Z' = 2), which differ considerably in their torsions involving the aliphatic urea nitrogen and carbonyl carbon atoms of each tripodal side arm, i.e., CH_2−CH_2−NH−(C═O) (Table S1 in the Supporting Information). In supramolecular chemistry, the existence of more than one molecular conformer in the same crystal structure has been described by the term *conformational isomorphism* and their occurrence enlightens concepts like kinetic and thermodynamic crystal stability because these are considered to be consequences of interrupted crystallization, as exemplified by Desiraju et al.[23] Crystal structure analysis of **L** reveals that both conformational isomorphs (**C1** and **C2**) are involved in intramolecular N−H···O hydrogen bonding between two arms of the receptor, which assist one of the aryl functions of hydrogen-bonded tripodal arms to be in closer proximity with the aryl ring of the third side arm, which is not involved in any intramolecular hydrogen bonding. The urea protons N2H and N3H of

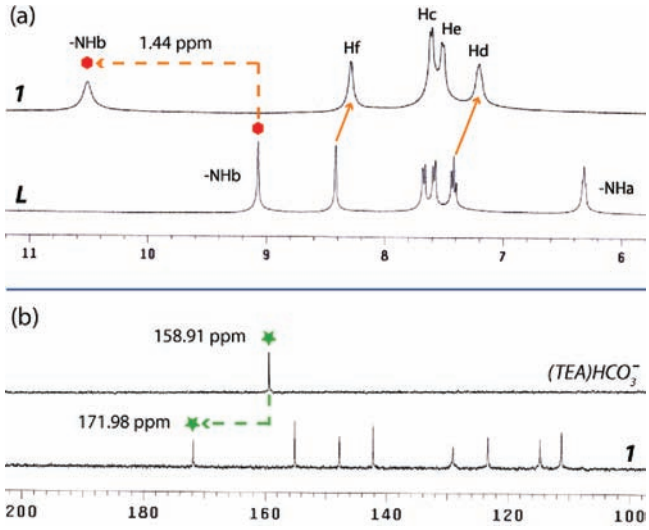

Figure 4. (a) Partial ^{1}H NMR spectrum of complex **1** (above) showing the spectral changes relative to receptor **L** (below). (b) Partial ^{13}C NMR spectrum of complex **1** (below) showing the huge downfield shift of the CO_3^{2-} resonance relative to the (TEA)HCO_3^- salt (above).

conformer **C1** and N12H and N13H of conformer **C2** are hydrogen-bonded to the amide oxygen atoms O7 and O16 in the respective conformers with a donor-to-acceptor distance of <3.0 Å, whereas the distances between the centroids of π-stacked phenyl rings are 3.882 Å (C2g···C3g) in conformer **C1** and 3.689 Å (C5g···C6g) in conformer **C2** (Figure 1a). Thus, the combined effect of intramolecular N−H···O hydrogen bonding and aromatic $\pi\cdots\pi$ stacking resists the opening of the tripodal side arms with a C_3 symmetry. Furthermore, each receptor unit is linked to two adjacent units of identical symmetry and of opposite orientation by intermolecular N−H···O hydrogen bonding, donated from the urea functions of π-stacked receptor side arms to the amide oxygen of adjacent inversion-symmetric molecules. The packing motif of **L**, as viewed down the crystallographic *b* axis, shows bilayer assembly formation among conformers of identical symmetry (Figure 1b), which are further linked to the molecules of adjacent bilayers (of different symmetry) through multiple C−H···O-(nitro) hydrogen bonds and C−H···π interactions (Figure 1c). The details of the intra- and intermolecular hydrogen-bonding interactions involved in the crystal structure of **L** are provided in Table S2 in the Supporting Information.

3.2. Carbonate-Encapsulated Complex (1). Good-quality crystals of *n*-tetrabutylammonium carbonate salt of the receptor **1** were obtained by slow evaporation of a DMSO solution of **L** in the presence of excess *n*-tetrabutylammonium fluoride (TBAF). Carbonate (CO_3^{2-}) was not present in the solution prior to crystallization, and we presume that the source of CO_3^{2-} is from the atmosphere where hydroxide ions generated in situ from the basic receptor/F^- solution dissolves aerial CO_2 into CO_3^{2-} at the air/solvent interface, resulting in the formation and crystallization of a CO_3^{2-}-entrapped dimeric capsule of **L**. Structural elucidation reveals that the in situ generated complex **1** crystallizes in the monoclinic system with centrosymmetric space group $C2/c$. Two symmetry-identical receptor molecules with opposite orientation form a capsular nanocavity that encapsulates a carbonate anion in its center (Figure 2a) via 12 N−H···O hydrogen bonds to the six urea functions and two aryl C−H···O interactions. The inversion-

dx.doi.org/10.1021/ic2020379 | *Inorg. Chem.* 2012, 51, 1727−1738

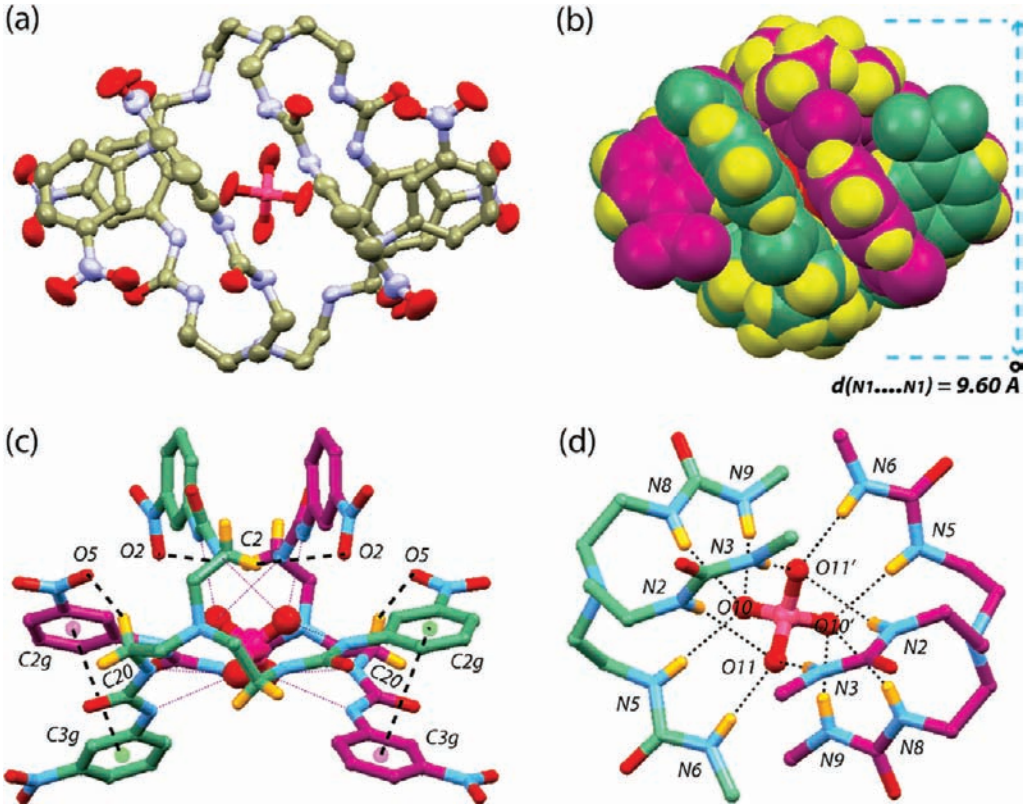

Figure 5. (a) Thermal ellipsoid plot (30% probability) of complex **2** depicting encapsulation of SO_4^{2-} within the centrosymmetric cage of two inversion-symmetric molecules of **L**. (b) Ball-and-stick representation depicting the intermolecular hydrogen-bonding interactions between the two receptor molecules of the SO_4^{2-}-entrapped dimeric capsule. (c) Spacefill representation depicting full encapsulation of the SO_4^{2-} anion. (d) Magnified view showing coordination of SO_4^{2-} with the 12 −NH protons of the dimeric capsule. TBA countercations are omitted for clarity of the presentation.

symmetric molecules are flipped inward toward each other in a face-to-face fashion with a distance of 9.058(3) Å between the apical nitrogen atoms (Figure 2b) and thereby generate a centrosymmetric molecular capsule assembled by aliphatic C−H···O(nitro) hydrogen bonds between each capsular unit. The carbonate oxygen atoms accept four N−H···O hydrogen bonds each, resulting in 12 hydrogen-bonding contacts with an average donor-to-acceptor (N···O) distance of 2.862 Å [d(N···O) = 2.781(3)−2.926(3) Å and ∠(N−H···O) = 164(2)−177(2)°; Table 2 and Figure 2c]. The urea protons N2H, N3H, N5H, and N6H from the individual coordinating receptor molecules donate one N−H···O hydrogen bond each to the carbonate oxygen atoms O11 and O11′, whereas N8H and N9H from each coordinating unit are N−H···O hydrogen-bonded to O10 of the carbonate anion (Figure 2d). In addition, the aryl proton C18H from each coordinating unit of the dimeric capsule makes contact with carbonate oxygen atoms O11 and O11′ via weak C−H···O interactions with a donor-to-acceptor (C···O) distance of 3.344(4) Å (Figure 2d). Thus, multiple (14) hydrogen-bonding interactions involving the urea −NH and aryl −CH protons provide high stability to the carbonate-encapsulated molecular capsule and serve as the foundation for efficient crystallization of the in situ formed complex. A correlation of the D−H···O angle versus the D−H···O (D = donor atom) distance shows that 10 out of 14 hydrogen bonds are in the strong hydrogen-bonding interaction regions of d(H···O) < 2.5 Å and d(D···O) < 3.2 Å (Table 2). TGA of the isolated crystals of **1** shows that the complex is stable up to 185 °C (Figure S9 in the Supporting Information).

Furthermore, the dimeric cages are interlinked with one another via weak aliphatic C−H···O(nitro) interactions to form a one-dimensional (1D) chain of capsular assemblies along the crystallographic a axis (Figure 3a). The packing diagram of **1** as viewed down the crystallographic c axis shows that the TBA cations are located between the 1D chains of hydrogen-bonding capsules via multiple aliphatic C−H···O-(nitro) interactions (Figure 3b).

The first evidence of CO_2 fixation using hydrogen-bonding receptors was reported by Gunnlaugsson et al. with a naphthalimide-based amine receptor, which in the presence of excess TBAF yielded a 1:1 receptor/HCO_3^- adduct from a DMSO solution.[14a] The second evidence of this class has been reported by Gale et al. with an amidourea macrocycle under identical crystallization conditions, to obtain crystals that proved to be a mixed tetrabutylammonium fluoride/carbonate salt, with the CO_3^{2-} anions bound within the macrocycle.[14c] The third example has recently been established by Ghosh et al. with a pentafluorophenyl-based tris(urea) receptor by crystallizing aerial CO_2 into a CO_3^{2-}-encapsulated dimeric capsule of the receptor from a 1:1 receptor/OH^- solution in DMSO.[14d] However, in the presence of fluoride ion (excess), the receptor has been found to encapsulate F^- via six hydrogen bonds to the three urea functions.[9d]

Thus, in order to validate the induction of hydroxide ions toward aerial CO_2 fixation, we attempted to grow crystals from an equimolar solution of **L** and (n-TBA)OH in DMSO. Slow evaporation of the solvent at room temperature yielded colorless crystals in a bulk amount within 1 or 2 days that

dx.doi.org/10.1021/ic2020379 | Inorg. Chem. 2012, 51, 1727−1738

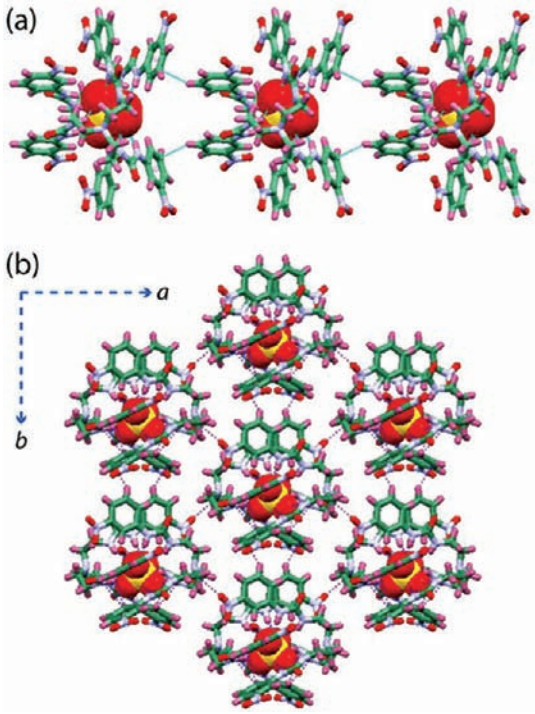

Figure 6. (a) Intermolecular C−H···π hydrogen-bonded 1D chain network of SO_4^{2-}-encapsulated molecular cages along the crystallographic *b* axis. (b) Crystal packing of complex **2** (as viewed down the *c* axis) showing the hexagonal arrangement of SO_4^{2-}-encapsulated dimeric cages around each capsular unit. TBA cations are omitted for clarity.

have proven to be complex **1**, as confirmed by powder XRD, FT-IR, and ^{1}H NMR analyses of the isolated crystals. The pattern of powder XRD analysis on bulk crystals isolated from the receptor/OH^- solution matches perfectly with the diffraction patterns of crystals of **1** obtained from the receptor/F^- solution, indicating the homogeneity of the isolated crystals of the carbonate complex (Figure S10 in the Supporting Information). It is remarkable to note that almost quantitative yield of **1** (above 90% based on **L**) can be obtained upon simple filtration/decantation of the crystals from the basic solution mixture (**L**/OH^- solution) after 3 days of exposure to an unmodified atmosphere, which indeed indicates the high affinity of **L** toward CO_2 fixation by encapsulation of the in situ generated CO_3^{2-} guest within the dimeric assembly of the receptor via multiple hydrogen bonds. A comparatively longer time duration observed in the crystallization of **1** from the receptor/F^- solution is presumably due to the slow generation of OH^- ions in a DMSO solution induced by excess F^- ions, which eventually fix atmospheric CO_2 at the air/solvent interface. Following the high affinity of **L** toward CO_2 fixation in a basic medium, efforts were made to grow crystals from a DMSO solution of **L** in the presence of alkali hydroxides (1 equiv of NaOH/KOH dissolved in a minimum quantity of water). However, in both cases, we ended up with crystals of **L** formed within a duration of 8−10 days, which was confirmed by powder XRD and FT-IR analyses of the isolated crystals (Figure S11 in the Supporting Information).

The ^{1}H NMR spectrum of complex **1** (DMSO-d_6) showed appreciable downfield shift and concomitant broadening of the urea $-NH_b$ resonance with a $\Delta\delta$ shift of 1.44 ppm, indicative of strong solution-state binding of CO_3^{2-} with the urea functions of **L** (Figure 4a). However, the resonance for the $-NH_a$ proton could not be observed presumably because of significant binding-induced broadening of the signals, as observed in the case of the $-NH_b$ proton. In addition, spectral changes have also been observed for the aliphatic $-NCH_2$ and aromatic protons (Ar−CH) of the receptor, which undergo a notable upfield shift ($\Delta\delta$ $-NCH_2$ = 0.12 ppm; $\Delta\delta$ ArH = 0.10−0.23 ppm) and get broadened upon recognition of the anion. This indeed indicates a solution-state structural alteration of the receptor side arms that could facilitate the formation of multiple N−H···O(anion) hydrogen bonds to encapsulate the carbonate guest within the C_3-symmetric cage of the receptor. CO_3^{2-} encapsulation has also been confirmed by monitoring the changes in the chemical shifts of ^{13}C NMR signals of a TEA salt of HCO_3^- and complex **1**. Tetraethylammonium bicarbonate in DMSO-d_6 showed a sharp ^{13}C NMR resonance at 158.91 ppm, whereas complex **1** showed a considerable downfield shift of the carbonate resonance at about 171.98 ppm ($\Delta\delta$ = 13.07 ppm), which may be attributed to the encapsulated CO_3^{2-} anion (Figure 4b). The presence of carbonate and the existence of strong N−H···O hydrogen bonds in complex **1** have also been established by solid-state FT-IR analysis. In the case of receptor **L**, the carbonyl (−C═O) stretching frequency is observed at 1655 cm^{-1}, whereas in complex **1**, it is observed at 1699 cm^{-1}, showing a huge shift of 44 cm^{-1} for the −C═O stretching relative to free **L** due to the formation of strong N−H···O hydrogen bonds with the carbonate oxygen atoms, as is evident from the structure of **1** (Figure S12 in the Supporting Information). The −NH stretching frequency of complex **1** (ν 3390 cm^{-1}) shows a considerable shift of 62 cm^{-1} with concomitant broadening of the peak in comparison to that of **L** (ν 3328 cm^{-1}), further demonstrating the existence of strong N−H···O hydrogen bonds between **L** and the CO_3^{2-} anion. Furthermore, the intense and strong peak at 2965 cm^{-1} may be attributed to C−H stretching of the TBA groups of complex **1**. In addition, a new peak is observed at 885 cm^{-1} in the fingerprint region of **1**, which can be attributed to the asymmetric stretching frequency of the carbonate anion.

3.3. Sulfate-Encapsulated Complex (2). The sulfate complex**2** was obtained as suitable crystals for XRD analysis upon the slow evaporation of a DMSO solution of **L** and excess *n*-tetrabutylammonium hydrogensulfate, which crystallizes in the monoclinic system with centrosymmetric space group *C*2/*c*. Crystal structure elucidation of **2** reveals that the hydrogensulfate anion has deprotonated and is bound in the form of SO_4^{2-} (divalent sulfate) by two inversion-symmetric units of **L** (Figure 5a), thereby creating a caged supramolecular structure assembled by weak aliphatic C−H···O(nitro) hydrogen bonds [C2···O2 = 3.625(7) Å, ∠C2−H2B···O2 = 150(3)° and C20···O5 = 3.522(7) Å, ∠C20−H20B···O5 = 135(3)°] and aromatic π···π interactions between the two identical receptor molecules [C13···C22 = 3.486(6) Å or C2g···C3g = 4.190 Å; Figure 5b]. Similar deprotonation of HSO_4^- has previously been observed by Ghosh et al. with a pentafluorophenyl-based tris(urea) receptor, which under identical crystallization conditions encapsulates SO_4^{2-} in a 2:1 (host/guest) ratio.[9d] Such solution-state deprotonation of the protonated state of an anion, viz., $H_2PO_4^-$, HCO_3^-, and HSO_4^-, is not uncommon and results because of the formation of multiple hydrogen-bonding interactions with the receptor that lower the pK_a of the bound guest to the extent that it is deprotonated by the free guest species in solution, and we presume the same process to occur

dx.doi.org/10.1021/ic2020379 | *Inorg. Chem.* 2012, 51, 1727−1738

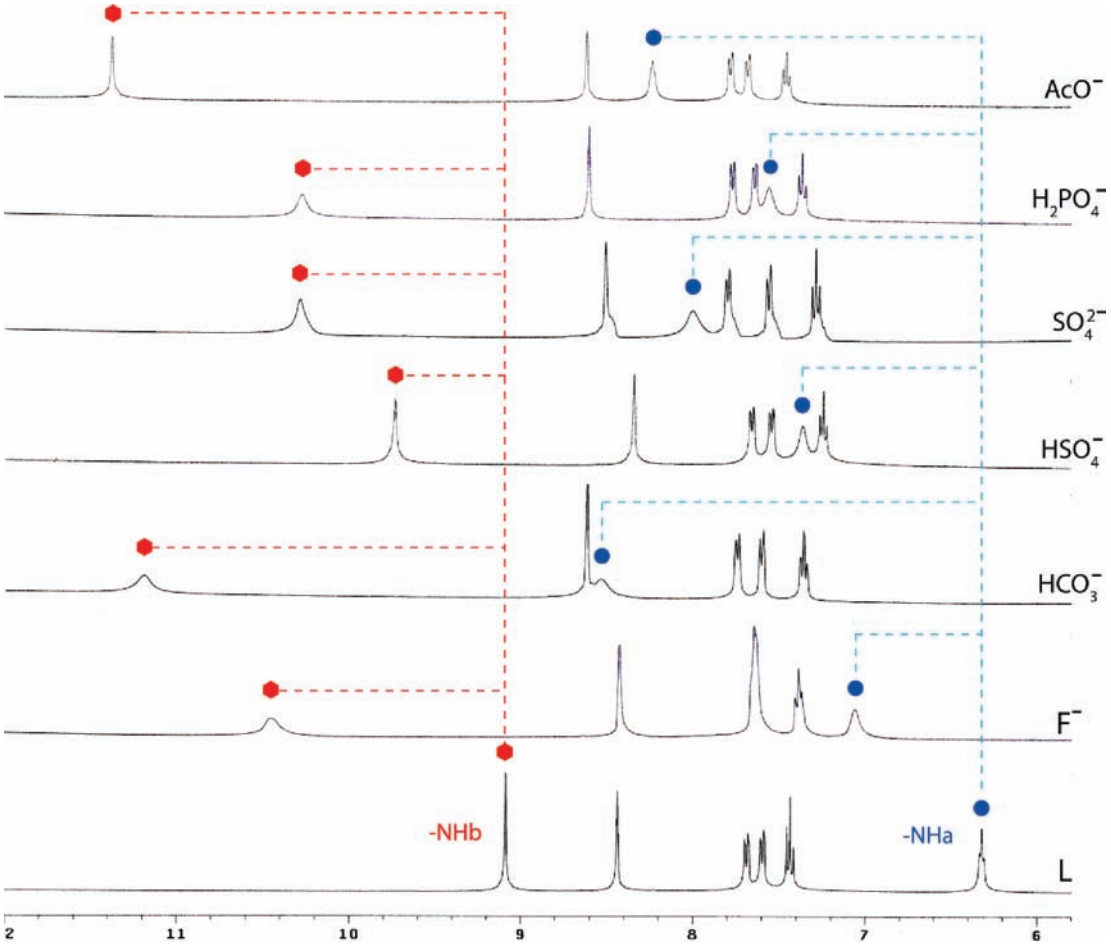

Figure 7. (a) Partial ^{1}H NMR spectra (400 MHz, DMSO-d_6) of **L** and maximum observable shifts of urea −NH resonances upon the addition of excess (5 equiv) F^-, HCO_3^-, HSO_4^-, SO_4^{2-}, $H_2PO_4^-$, and AcO^- as their TEA/TBA salts. The quaternary ammonium salts were added at once to the individual solutions of **L**.

Table 3. Binding Constants (log *K*) of L with Various Anions in DMSO-d_6

anion	log *K*	anion	log *K*
HCO_3^-	4.14	$H_2PO_4^-$	4.38
F^-	3.87	AcO^-	3.27
HSO_4^-	4.52	NO_3^-	no binding
SO_4^{2-}	4.78	ClO_4^-	no binding

here, as suggested by Gale et al.[24] The inversion-symmetric molecules of **L** are flipped inward toward each other in a face-to-face fashion [d(N1···N1) = 9.602(4) Å; Figure 5c], forming a centrosymmetric molecular cage that encapsulates a sulfate anion in its center via 12 N−H···O hydrogen bonds to the six urea functions with an average donor-to-acceptor (N···O) distance of 2.862 Å (Table 2). Each sulfate oxygen atom behaves as a trifurcated hydrogen-bond acceptor and each −NH group donates one N−H···O bond (Figure 5d), resulting in 12 hydrogen bonds, which is consistent with the electronic structure calculations by Hay et al. suggesting that each oxoanion oxygen atom could be involved in a maximum of three hydrogen bonds.[25] Thus, the structure reported here represents the optimal coordination number for the sulfate anion. The urea protons N5H, N8H, and N9H from individual coordinating receptor molecules of the dimeric capsule are hydrogen-bonded to sulfate oxygen atoms O10 and O10′, whereas O11 and O11′ are hydrogen-bonded to both receptor molecules by urea protons N2H, N3H, and N6H, where N2H and N6H from one coordinating unit and N3H from the other unit provide a three-point coordination to O11/O11′ (Figure 5d). A similar type of binding has previously been reported by Custelcean et al. for SO_4^{2-} encapsulation by the silver MOF complex derived from an identical tris(urea) scaffold.[9g] A correlation of the N−H···O angle versus the N−H···O distance shows that 10 out of 12 hydrogen bonds are in the strong hydrogen-bonding interaction regions of d(H···O) < 2.5 Å and d(N···O) < 3.2 Å, which perhaps contributes to the high stability of **2** (mp = 242 °C), as is evident from TGA of the isolated crystals of **2** (Figure S15 in the Supporting Information). Furthermore, the sulfate-encapsulated dimeric cages are interlinked with one another via weak aromatic C−H···π interactions (C8···C3g = 3.897 Å; ∠C8−H···C3g = 138°) to form a 1D chain of capsular assemblies along the crystallographic b axis (Figure 6a). Two such 1D arrays of capsular assemblies are further interconnected with one another by weak aliphatic C−H···O(nitro) interactions [C19···O3 = 3.155(7) Å; ∠C19−H···O3 = 107(3)°], generating hexagonal networks of sulfate-encapsulated dimeric cages around each capsular unit (Figure 6b). In addition, multiple C−H···O(nitro) interactions formed between the *n*-TBA counteractions and nitro groups of the receptor side arms provide increased stability to the caged supramolecular assembly formation.

dx.doi.org/10.1021/ic2020379 | *Inorg. Chem.* 2012, 51, 1727−1738

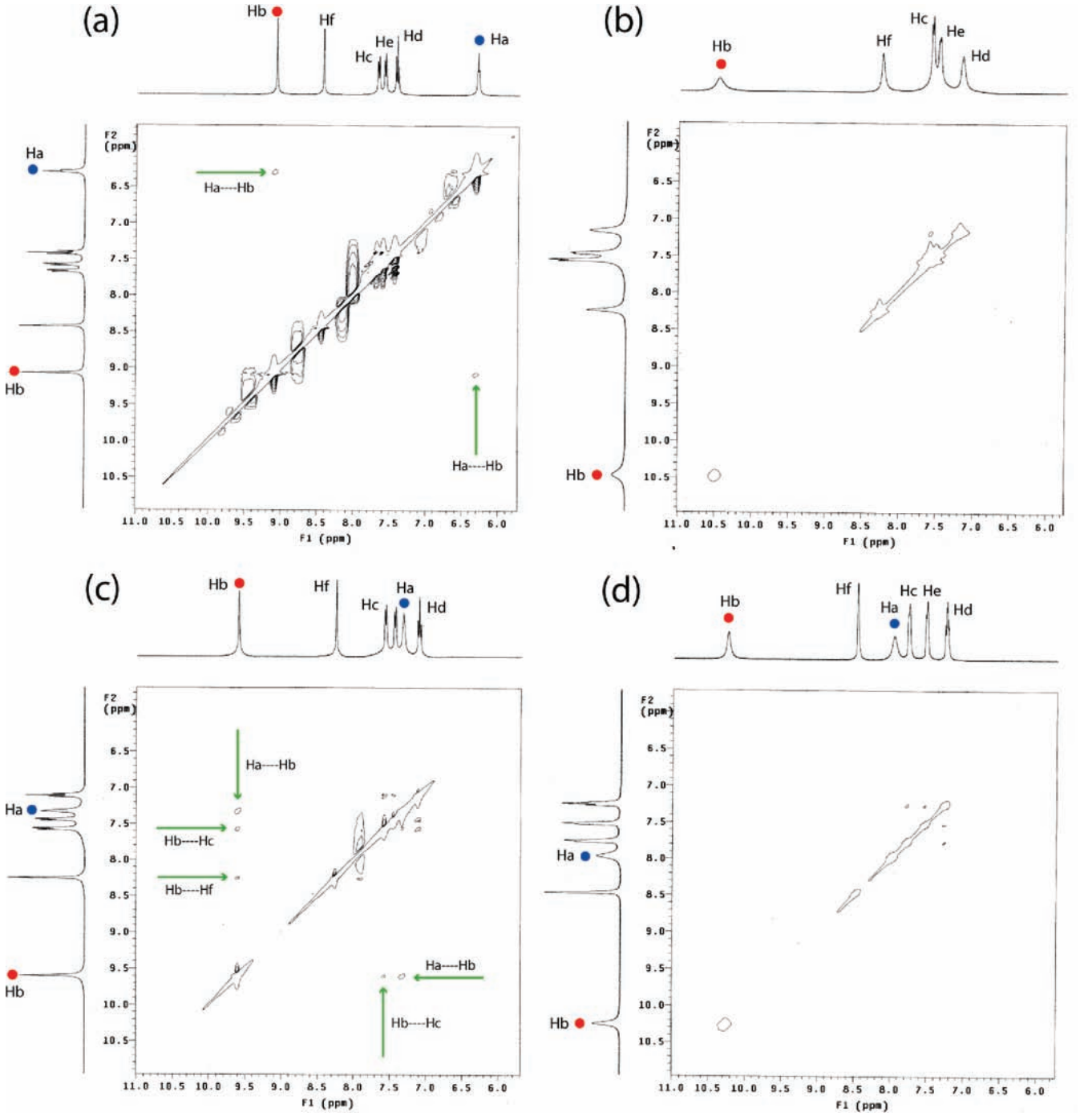

Figure 8. 2D NOESY NMR experiments of (a) free receptor **L**, (b) carbonate complex **1**, (c) sufate complex **2**, and (d) **L** in the presence of excess sulfate (5 equiv) in DMSO-d_6.

It is important to mention here that attempted crystallization of a DMSO or MeCN solution of **L** in the presence of excess $(TBA)_2SO_4^{2-}$ (50 wt % solution in water) was not fruitful, presumably because of the high moisture content of the receptor/anion solution and the capability of protic solvents to compete for SO_4^{2-} along with urea −NH functions of **L**, disfavoring the formation of a SO_4^{2-}-encapsulated molecular capsule. However, encapsulation of a sulfate/water/sulfate adduct within the dimeric capsule of a positional isomer of **L** (*p*-nitrophenyl derivative) has been reported from identical crystallization conditions (MeCN/water) with a 1:1 receptor to anion binding.[9b]

The presence of sulfate in complex **2** and its coordination via strong N−H···O hydrogen bonds has also been confirmed by solid-state FT-IR analysis (Figure S16 in the Supporting Information). In complex **2**, the amide (−C═O) stretching frequency is observed at 1695 cm^{-1}, showing a considerable shift of 40 cm^{-1} relative to free **L** due to the formation of strong NH···O hydrogen bonds with the sulfate oxygen atoms (Figure S17 in the Supporting Information). Additional information regarding the existence of strong N−H···O hydrogen bonds between **L** and SO_4^{2-} can be obtained by examining the −NH peak of the spectrum, which gets broadened in **2** relative to **L** with an observable shift of 12 cm^{-1}. Furthermore, the intense

dx.doi.org/10.1021/ic2020379 | *Inorg. Chem.* 2012, 51, 1727−1738

and strong peak at 2963 cm^{-1} may be attributed to C−H stretching of the TBA groups in complex **2**. In addition, a new peak is observed at 1089 cm^{-1} in complex **2**, which can be attributed to the symmetric stretching frequency of the sulfate anion. Typically, the symmetric absorption (1089 cm^{-1}) is intense and broad and most often does exist as multiple band structures as observed for **2**, and this may be used to characterize the presence of sulfate in individual compounds/complexes. Furthermore, the ^{1}H NMR spectrum of complex **2** (DMSO-d_6) showed a significant downfield shift of the −NH resonances with a $\Delta\delta$ value of 1.02 and 0.51 ppm for $-NH_a$ and $-NH_b$ protons, respectively (Figure S18 in the Supporting Information). Additionally, the aliphatic $-NCH_2$ and aromatic protons (Ar−CH) of the receptor experience a noticeable upfield shift ($\Delta\delta$ $-NCH_2$ = 0.15 ppm; $\Delta\delta$ ArH = 0.20−0.31 ppm), suggestive of a structural alteration of **L** in solution that could influence the urea functions from each receptor side arm to encapsulate the sulfate anion within the tripodal pseudocavity by multiple N−H···O hydrogen bonds.

3.4. Solution-State Anion-Binding Studies. Solution-state binding properties of **L** were carried out with TEA/HCO_3^- and *n*-TBA salts of F^-, AcO^-, $H_2PO_4^-$, HSO_4^-, and SO_4^{2-} by qualitative as well as quantitative ^{1}H NMR experiments in DMSO-d_6. Figure 7 represents the qualitative test of anions, which shows the chemical shift changes observed upon the excess addition of different anions to the urea receptor **L** in DMSO-d_6. The most significant changes have been observed for the urea protons ($-NH_a$ and $-NH_b$), indicating that the −NH functions provide the primary sites of interaction between the ligand and anions. In the quantitative ^{1}H NMR titration of **L** with a standard HCO_3^- solution, a large downfield shift of urea −NH resonances with an average $\Delta\delta$ value of 1.48 ppm ($\Delta\delta$ $-NH_a$ = 1.51 ppm; $\Delta\delta$ $-NH_b$ = 1.45 ppm) and a notable upfield shift of aromatic −CH signals were observed. Following the shift of the −NH signal, the association constant (log *K*) for HCO_3^- was calculated to be 4.14 with a 1:1 host/guest stoichiometry, in agreement with Job's plot analysis (Figures S19 and S20 in the Supporting Information). The titration data for F^- as well gave the best fit for 1:1 stoichiometry with a log *K* value of 3.87 (Figure S21 in the Supporting Information). The considerably larger shift of $-NH_b$ ($\Delta\delta$ = 1.44 ppm) relative to $-NH_a$ signals ($\Delta\delta$ = 0.89 ppm) suggests that F^- is bound more strongly to $-NH_b$ than $-NH_a$ protons of the receptor (Figure S22 in the Supporting Information). However, in a proof-of-concept experiment, when the titrated receptor/F^- solution (1:10 host/guest) was bubbled with CO_2 for about 5 min (100 mL min^{-1}), immediate ^{1}H NMR analysis showed a further downfield shift of the $-NH_a$ resonance ($\Delta\delta$ = 1.42 ppm with respect to **L**), indicating the in situ formation of carbonate/bicarbonate in the presence of excess F^- ions. Furthermore, ^{1}H NMR titration of **L** with standard SO_4^{2-} and HSO_4^- solutions led to the best fit for 1:1 stoichiometry of host to guest, in agreement with Job's plot analyses (Figures S23 and S24 in the Supporting Information), whereas the single-crystal XRD analysis of complex **2** showed a 2:1 host/guest binding for the divalent sulfate anion. Such a binding discrepancy in the solid and solution states is not uncommon. In the solid state, the receptor is more organized and prefers binding and encapsulation of the oxyanion within the dimeric cage structure of the receptor stabilized by several hydrogen-bonding interactions, whereas binding of a single anion inside the receptor cavity has been observed in solution. The association constants (log *K*) of **L** with SO_4^{2-} and HSO_4^- were calculated to be 4.78 and 4.52. The identical modes of binding (1:1 host/guest) and association constants of $K > 10^4$ M^{-1} calculated using both sulfate and bisulfate indicate that in solution bisulfate gets converted to sulfate in our experimental conditions, which indeed supports the solid-state formation of the SO_4^{2-}-encapsulated complex **2** when **L** is treated with excess *n*-TBA salt of HSO_4^- in DMSO. Additionally, the chemical shifts of the urea −NH signals in the presence of 1 equiv of SO_4^{2-} and HSO_4^- have been found to be almost the same (in the case of SO_4^{2-}, $\Delta\delta$ $-NH_a$ = 1.18 ppm and $-NH_b$ = 0.72 ppm, and in the case of HSO_4^-, $\Delta\delta$ $-NH_a$ = 1.13 ppm and $-NH_b$ = 0.71 ppm) and closely resemble those in the ^{1}H NMR spectrum for the isolated crystals of **2** (Figures S25 and S26 in the Supporting Information). In our recent communication, we have shown the in situ generation of a PO_4^{3-}-encapsulated rigidified cage structure of a tris(thiourea) receptor obtained via hydrogen-bond-induced deprotonation of bound $H_2PO_4^-$ by free $H_2PO_4^-$, which is evident from the origin of new sets of signals (for −NH and ArH protons) in the ^{1}H NMR titration experiments.[16b] However, in the case of the tris(urea) receptor **L**, no new resonances corresponding to the −NH and/or ArH protons were observed during ^{1}H NMR titration with HSO_4^-, presumably almost identical $\Delta\delta$ shifts of the −NH resonances induced by the addition of HSO_4^- and SO_4^{2-} ions. A comparatively larger downfield shift of the aliphatic $-NH_a$ signal relative to the aryl $-NH_b$ signal suggests that in solution SO_4^{2-}/HSO_4^- is bound more strongly to $-NH_a$ than $-NH_b$ protons of the receptor, which is in contrast to the X-ray structure of the sulfate complex (**2**), which shows equal participation from both the urea protons toward SO_4^{2-} binding within the dimeric cage of **L** (Table 2). Similar to the HCO_3^- titration experiment, increasing the addition of a standard $H_2PO_4^{2-}$ solution results in an identical downfield shift of both −NH signals with an average $\Delta\delta$ value of 1.42 ppm ($\Delta\delta$ $-NH_a$ = 1.43 ppm; $\Delta\delta$ $-NH_b$ = 1.42 ppm), indicative of equal and active participation of both urea protons toward binding of this anion in a 1:1 stoichiometry (**L**/$H_2PO_4^-$) with an association constant of 4.38 (Figures S27 and S28 in the Supporting Information). Finally, in ^{1}H NMR titration of **L** with a standard CH_3COO^- solution, the −NH resonance experiences a huge downfield shift with ultimate $\Delta\delta$ values of 2.08 and 2.42 ppm for the $-NH_a$ and $-NH_b$ signals, respectively, suggestive of equal and strong participation of the −NH protons toward binding of this anion in a 1:1 stoichiometry with an association constant (log *K*) of 3.27 (Figures S29 and S30 in the Supporting Information). However, in the presence of other oxyanions such as nitrate and perchlorate, no appreciable changes in the chemical shift values of the −NH resonances were observed, suggesting the noninteracting nature or very weak interactions with **L**. The association constants (log *K*) calculated by following the shift of the most deshielded urea proton ($-NH_a$ or $-NH_b$) of **L** in the ^{1}H NMR titration experiments with different anions (Table 3) are comparable to those observed for the *p*-nitrophenyl-,[9b] pentafluorophenyl-,[9d] or *p*-cyanophenyl[9l]-substituted tris(urea) receptors.

The solution-state encapsulation of oxyanions has further been confirmed by 2D NOESY NMR experiments of the isolated complexes (**1** and **2**) and free receptor (**L**) in DMSO-d_6 (Figure 8). As depicted in Figure 8a, the free receptor molecule showed a strong NOESY signal between the urea protons $-NH_a$ and $-NH_b$, whereas such $H_a\cdots H_b$ interactions were found to be absent in complex **1** (Figure 8b), indicating the binding and encapsulation of carbonate within the tripodal

dx.doi.org/10.1021/ic2020379 | Inorg. Chem. 2012, 51, 1727−1738

scaffold in a 2:1 host/guest stoichiometry, an observation that is also supported by the X-ray structure of the carbonate-encapsulated dimeric cage of **L** (**1**). In contrast, two strong NOESY signals between $H_a\cdots H_b$ and $H_b\cdots H_c$ protons have been observed in complex **2** (Figure 8c), which indeed suggests that the 2:1 host/guest stoichiometry is not the prevalent mode of sulfate binding in solution. However, upon further addition of sulfate ions to the solution of **2** in DMSO-d_6, the NOESY signals between $H_a\cdots H_b$ and $H_b\cdots H_c$ disappeared, indicating a conformational change of the receptor due to encapsulation of a sulfate anion in a 1:1 host/guest ratio (Figure 8d). Similarly, in the presence of excess bicarbonate ions, no signals due to $H_a\cdots H_b$ or $H_b\cdots H_c$ interactions have been observed, suggesting the binding and encapsulation of bicarbonate within the receptor scaffold (Figure S31 in the Supporting Information). The 1:1 binding stoichiometry of sulfate and bicarbonate was further established by Job's plot analysis from the ^{1}H NMR titration experiments, showing a maximum at 0.5 mole fraction of **L**. Similar NOESY NMR experiments have recently been reported by Hossain et al. for bisulfate encapsulation by a tren-based urea receptor.[91]

4. CONCLUSION

In conclusion, we have demonstrated the efficient fixation of aerial CO_2 in the form of air-stable crystals of a carbonate-encapsulated molecular capsule of a simple tris(urea) receptor, **L**. The in situ generated carbonate anion is bound within a centrosymmetric dimeric cage of the receptor with an array of 12 N−H···O and 2 C−H···O hydrogen bonds. The fixation process can reproducibly be accomplished from a DMSO solution of the receptor charged either with an equivalent amount of hydroxide ions or an excess of fluoride ions. It is remarkable to note that almost quantitative conversion of **L** to the carbonate-encapsulated complex (**1**) can be obtained from the basic receptor/OH^- solution, which establishes **L** as a potential hydrogen-bonding scaffold for the effective fixation of atmospheric CO_2. In addition, we have also demonstrated the structural evidence for encapsulation of a deprotonated hydrogensulfate anion (SO_4^{2-}) within a fully complementary centrosymmetric dimeric assembly of the receptor via 12 N−H···O hydrogen bonds (**2**). Thus, receptor **L** provides an excellent case of understanding the significance of hydrogen-bonding tripodal scaffolds toward the formation of oxyanion-encapsulated caged supramolecular frameworks by in situ generation of the bound anionic species.

■ ASSOCIATED CONTENT

Supporting Information

Crystallographic files in CIF format, additional crystallographic data, characterization data, and ^{1}H NMR titration spectra. This material is available free of charge via the Internet at http://pubs.acs.org.

■ AUTHOR INFORMATION

Corresponding Author

*E-mail: gdas@iitg.ernet.in.

■ ACKNOWLEDGMENTS

G.D. gratefully acknowledges DST (SR/S1/IC-01/2008) and CSIR (01-2235/08/EMR-II) New Delhi, India, for financial support and DST-FIST for its single-crystal XRD facility and Central Instrument Facility at IIT Guwahati. S.K.D. acknowledges IIT Guwahati, India, for a senior research fellowship.

■ REFERENCES

(1) (a) Bowman-James, K. *Acc. Chem. Res.* **2005**, *38*, 671−678. (b) Gale, P. A.; Garcia-Garrido, S. E.; Garric, J. *Chem. Soc. Rev.* **2008**, *37*, 151−190. (c) Caltagirone, C.; Gale, P. A. *Chem. Soc. Rev.* **2009**, *38*, 520−563. (d) Sessler, L.; Gale, P. A.; Cho, W. S. In *Anion Receptor Chemistry: Monographs in Supramolecular Chemistry*; Stoddart, J. F., Ed.; Royal Society of Chemistry: Cambridge, U.K., 2006. (e) Themed issue: Supramolecular chemistry of anionic species . *Chem. Soc. Rev.* **2010**, *39*, 3581. (f) Schottel, B. L.; Chifotides, H. T.; Dunbar, K. R. *Chem. Soc. Rev.* **2008**, *37*, 68−83.

(2) (a) Kang, S. O.; Begum, R. A.; Bowman-James, K. *Angew. Chem., Int. Ed.* **2006**, *45*, 7882−7894. (b) Kang, S. O.; Hossain, M. A.; Bowman-James, K. *Coord. Chem. Rev.* **2006**, *250*, 3038−3052. (c) Arunachalam, M.; Ghosh, P. *Chem. Commun.* **2009**, 5389−5391. (d) Arunachalam, M.; Ghosh, P. *Inorg. Chem.* **2010**, *49*, 943−951. (e) Valiyaveettil, S.; Engbersen, J. F. J.; Verboom, W.; Reinhoudt, D. N. *Angew. Chem., Int. Ed. Engl.* **1993**, *32*, 900−901. (f) Choi, K.; Hamilton, A. D. *J. Am. Chem. Soc.* **2001**, *123*, 2456−2457. (g) Liao, J.-H.; Chen, C.-T.; Fang, J. M. *Org. Lett.* **2002**, *42*, 561−564. (h) Kondo, S.-I.; Hiraoka, Y.; Kurumatani, N.; Yano, Y. *Chem. Commun.* **2005**, 1720−1722. (i) Beer, P. D.; Dickson, A. P.; Fletcher, N.; Goulden, A. J.; Grieve, A.; Hodacova, J.; Wear, T. *J. Chem. Soc., Chem. Commun.* **1993**, 828−830.

(3) (a) Steed, J. W. *Chem. Soc. Rev.* **2010**, *39*, 3686−3699. (b) Li, A.-F.; Wang, J.-H.; Wang, F.; Jiang, Y.-B. *Chem. Soc. Rev.* **2010**, *39*, 3729−3745. (c) Amendola, V.; Fabbrizzi, L.; Mosca, L. *Chem. Soc. Rev.* **2010**, *39*, 3889−3915. (d) *The Encyclopedia of Supramolecular Chemistry*; Atwood, J. L., Steed, J. W., Eds.; Marcel Dekker: New York, 2004. (e) Bondy, C. R.; Loeb, S. J. *Coord. Chem. Rev.* **2003**, *240*, 77−99. (f) Li, M.; Hao, Y.; Wu, B.; Jia, C.; Huang, X.; Yang, X.-J. *Org. Biomol. Chem.* **2011**, *9*, 5637−5640.

(4) (a) Gale, P. A.; Sessler, J. L.; Camiolo, S. In *Encyclopedia of Supramolecular Chemistry*; Atwood, J. L., Steed, J. W., Ed.; Marcel Dekker: New York, 2004; pp 1176−1185. (b) Yu, J. G.; Lei, M.; Cheng, B.; Zhao, X. J. *J. Solid State Chem.* **2004**, *177*, 681−689. (c) Vega, I. E. D.; Gale, P. A.; Hursthouse, M. B.; Light, M. E. *Org. Biomol. Chem.* **2004**, *2*, 2935−2941. (d) Sessler, J. L.; Barkey, N. M.; Pantos, G. D.; Lynch, V. M. *New J. Chem.* **2007**, *31*, 646−654. (e) Yoo, J.; Kim, M.; Hong, S.; Sessler, J. L.; Lee, C. *J. Org. Chem.* **2009**, *74*, 1065−1069. (f) Sessler, J. L.; Cai, J.; Gong, H.; Yang, X.; Arambula, J. F.; Hay, B. P. *J. Am. Chem. Soc.* **2010**, *132*, 14058−14060.

(5) (a) Gale, P. A. *Chem. Commun.* **2008**, 4525−4540. (b) Sessler, J. L.; Cho, D.-G.; Lynch, V. *J. Am. Chem. Soc.* **2006**, *128*, 16518−16519. (c) Gale, P. A.; Hiscock, J. R.; Jie, C. Z.; Hursthouse, M. B.; Light, M. E. *Chem. Sci.* **2010**, 215−220. (d) Bates, G. W.; Triyanti.; Light, M. E.; Albrecht, M.; Gale, P. A. *J. Org. Chem.* **2007**, *72*, 8921−8927.

(6) (a) Arunachalam, M.; Ghosh, P. *Chem. Commun.* **2011**, *47*, 8477−8492. (b) Arunachalam, M.; Ghosh, P. *Chem. Commun.* **2011**, *47*, 6269−6271. (c) Arunachalam, M.; Ghosh, P. *Org. Lett.* **2010**, *12*, 328−331. (d) Arunachalam, M.; Ahamed, B. N.; Ghosh, P. *Org. Lett.* **2010**, *12*, 2742−2745. (e) Gale, P. A. *Acc. Chem. Res.* **2006**, *39*, 465−475.

(7) (a) Atwood, J. L.; Szumna, A. *J. Am. Chem. Soc.* **2002**, *124*, 10646−10647. (b) Wu, A.; Isaacs, L. *J. Am. Chem. Soc.* **2003**, *125*, 4831−4835. (c) Shivanyuk, A.; Rebek, J. Jr. *J. Am. Chem. Soc.* **2003**, *125*, 3432−3433. (d) Yamauchi, Y.; Fujita, M. *Chem. Commun.* **2010**, *46*, 5897−5899. (e) Ikemoto, K.; Inokuma, Y.; Fujita, M. *Angew. Chem., Int. Ed.* **2010**, *49*, 5750−5752. (f) Yoshizawa, M.; Klosterman, J. K.; Fujita, M. *Angew. Chem., Int. Ed.* **2009**, *48*, 3418−3438. (g) Rebek, J. Jr. *Chem. Commun.* **2000**, 637−643. (h) Hof, F.; Craig, S. L.; Nuckolls, C.; Rebek, J. Jr. *Angew. Chem., Int. Ed.* **2002**, *41*, 1488−1508.

(8) (a) Moyer, B. A.; Bonnesen, P. V. In *Physical factors in anion separation, Supramolecular chemistry of anions*; Bianchi, A., Bowman-James, K., Garcia-Espana, E., Eds.; Wiley-VCH: New York, 1997. (b) Wang, X. B.; Yang, X.; Nicholas, J. B.; Wang, L. S. *Science* **2001**,

294, 1322. (c) McKee, M. L. *J. Phys. Chem.* **1996**, *100*, 3473−3481. (d) Blades, A. T.; Kebarle, P. *J. Am. Chem. Soc.* **1994**, *116*, 10761−10766.

(9) (a) Jia, C.; Wu, B.; Li, S; Huang, X.; Zhao, Q.; Li, Q.-S.; Yang, X.-J. *Angew. Chem., Int. Ed.* **2011**, *50*, 486−490. (b) Jose, D. A.; Kumar, D. K.; Ganguly, B.; Das, A. *Inorg. Chem.* **2007**, *46*, 5817−5819. (c) Ravikumar, I.; Ghosh, P. *Chem. Commun.* **2010**, *46*, 6741−6743. (d) Ravikumar, I.; Lakshminarayanan, P. S.; Arunachalam, M.; Suresh, E.; Ghosh, P. *Dalton Trans.* **2009**, 4160−4168. (e) Custelcean, R.; Remy, P.; Bonnesen, P. V.; Jiang, D.-E.; Moyer, B. A. *Angew. Chem., Int. Ed.* **2008**, *47*, 1866−1870. (f) Lakshminarayanan, P. S.; Ravikumar, I.; Suresh, E.; Ghosh, P. *Chem. Commun.* **2007**, 5214−5216. (g) Custelcean, R.; Moyer, B. A.; Hay, B. P. *Chem. Commun.* **2005**, *47*, 5971−5973. (h) Custelcean, R.; Remy, P. *Cryst. Growth. Des.* **2009**, *9*, 1985−1989. (i) Wu, B.; Liang, J.; Yang, J.; Jia, C.; Yang, X.-J.; Zhang, H.; Tang, N.; Janiak, C. *Chem. Commun.* **2008**, 1762−1764. (j) Busschaert, N.; Wenzel, M.; Light, M. E.; Iglesias-Hernandez, P.; Perez-Tomas, R.; Gale, P. A. *J. Am. Chem. Soc.* **2011**, *133*, 14136−14148. (k) Busschaert, N.; Gale, P. A.; Haynes, C. J. E.; Light, M. E.; Moore, S. J.; Tong, C. C.; Davis, J. T.; Harrell, W. A. Jr. *Chem. Commun.* **2010**, *46*, 6252−6254. (l) Pramanik, A.; Thompson, B.; Hayes, T.; Tucker, K.; Powell, D. R.; Bonnesen, P. V.; Ellis, E. D.; Lee, K. S.; Yu, H.; Hossain, M. A. *Org. Biomol. Chem.* **2011**, *9*, 4444−4447.

(10) (a) Sessler, J. L.; Katayev, E.; Pantos, G. D.; Ustynyuk, Y. A. *Chem. Commun.* **2004**, 1276−1278. (b) Eller, L. R.; Stepien, M.; Fowler, C. J.; Lee, J. T.; Sessler, J. L.; Moyer, B. A. *J. Am. Chem. Soc.* **2007**, *129*, 11020−11021. (c) Fowler, C. J.; Haverlock, T. J.; Moyer, B. A.; Shriver, J. A.; Gross, D. E.; Marquez, M.; Sessler, J. L.; Hossain, M. A.; Bowman-James, K. *J. Am. Chem. Soc.* **2008**, *130*, 14386−4387. (d) Moyer, B. A.; Delmau, L. H.; Fowler, C. J.; Ruas, A.; Bostick, D. A.; Sessler, J. L.; Katayev, E.; Pantos, G. D.; Llinares, J. M.; Hossain, M. A.; Kang, S. O.; Bowman-James, K. *Adv. Inorg. Chem.* **2007**, *59*, 175−204.

(11) Pflugrath, J. W.; Quiocho, F. A. *Nature* **1985**, *314*, 257−260.

(12) (a) Climate Change 2007: *Synthesis Report, International Panel on Climate Change*; Cambridge University Press: Cambridge, U.K., 2007. (b) Jenkinson, D. S.; Adams, D. E.; Wild, A. *Nature* **1991**, *351*, 304−306. (c) Caldeira, K.; Jain, A. K.; Hoffert, M. I. *Science* **2003**, *299*, 2052−2054. (d) Aresta, M.; Dibendetto, A. *Dalton Trans.* **2007**, 2975−2992. (e) Olah, G. A.; Goeppert, A.; Prakash, G. K. S. *J. Org. Chem.* **2009**, *74*, 487−498.

(13) (a) Banerjee, R.; Phan, A.; Wang, B.; Knobler, C.; Furukawa, H.; O'Keeffe, M.; Yaghi, O. M. *Science* **2008**, *319*, 939−943. (b) Rowsell, J. L. C.; Spencer, E. C.; Eckert, J.; Howard, A. K.; Yaghi, O. M. *Science* **2005**, *309*, 1350−1354. (c) Momming, C. M.; Otten, E.; Kehr, G.; Frohlich, R.; Grimme, S.; Stephan, D. W.; Erker, G. *Angew. Chem., Int. Ed.* **2009**, *48*, 6643−6646. (d) Olah, G. A. *Angew. Chem., Int. Ed.* **2005**, *44*, 2636−2640. (e) Kong, L.-Y.; Zhang, Z.-H.; Zhu, H.-F.; Kawaguchi, H.; Okamura, T.-A.; Doi, M.; Chu, Q.; Sun, W.-Y.; Ueyama, N. *Angew. Chem., Int. Ed.* **2005**, *44*, 4352−4355. (f) Garcia-Espana, E.; Gavina, P.; Latorre, J.; Soriano, C.; Verdejo, B. *J. Am. Chem. Soc.* **2004**, *126*, 5082−5083. (g) Mao, Z. W.; Liehr, G.; Van Eldik, R. *J. Am. Chem. Soc.* **2000**, *122*, 4839−4840.

(14) (a) Gunnlaugsson, T.; Kruger, P. E.; Jensen, P.; Pfeffer, F. M.; Hussey, G. M. *Tetrahedron Lett.* **2003**, *44*, 8909−8913. (b) Brooks, S. J.; Garcia-Garrido, S. E.; Light, M. E.; Cole, P. A.; Gale, P. A. *Chem.—Eur. J.* **2007**, *13*, 3320−3329. (c) Brooks, S. J.; Gale, P. A.; Light, M. E. *Chem. Commun.* **2006**, 4344−4346. (d) Ravikumar, I.; Ghosh, P. *Chem. Commun.* **2010**, *46*, 1082−1084.

(15) (a) Edwards, P. R.; Hiscock, J. R.; Gale, P. A. *Tetrahedron Lett.* **2009**, *50*, 4922−4924. (b) Edwards, P. R.; Hiscock, J. R.; Gale, P. A.; Light, M. E. *Org. Biomol. Chem.* **2010**, *8*, 100−106.

(16) (a) Dey, S. K.; Das, G. *Chem. Commun.* **2011**, *47*, 4983−4985. (b) Dey, S. K.; Das, G. *Dalton Trans.* **2011**, *40*, 12048−12051. (c) Dey, S. K.; Das, G. *Cryst. Growth Des.* **2011**, *11*, 4463−4473. (d) Dey, S. K.; Ojha, B.; Das, G. *CrystEngComm* **2011**, *13*, 269−278. (e) Dey, S. K.; Pramanik, A.; Das, G. *CrystEngComm* **2011**, *13*, 1664−1675. (f) Pramanik, A.; Das, G. *Tetrahedron Lett.* **2009**, *65*, 2196−2200.

(17) Mendy, J. S.; Pilate, M. L.; Horne, T.; Day, V. W.; Hossain, M. A. *Chem. Commun.* **2010**, *46*, 6084−6086.

(18) *SMART, SAINT, and XPREP*; Siemens Analytical X-ray Instruments Inc.: Madison, WI, 1995.

(19) Sheldrick, G. M. *SADABS: Software for Empirical Absorption Correction*; Institute fur Anorganische Chemieder Universitat, University of Gottingen: Gottingen, Germany, 1999−2003.

(20) Sheldrick, G. M. *SHELXS-97*; University of Gottingen: Gottingen, Germany, 1997.

(21) Sheldrick, G. M. *SHELXL-97: Program for Crystal Structure Refinement*; University of Gottingen: Gottingen, Germany, 1997.

(22) *Mercury 2.3, Supplied with Cambridge Structural Database*; CCDC: Cambridge, U.K., 2010.

(23) Desiraju, G. R. *Angew. Chem, Int. Ed.* **2007**, *46*, 8342−8356.

(24) (a) Caltagirone, C.; Hiscock, J. R.; Hursthouse, M. B.; Light, M. E.; Gale, P. A. *Chem.—Eur. J* **2008**, *14*, 10236−10243. (b) Gale, P. A.; Hiscock, J. R.; Moore, S. J.; Caltagirone, C.; Hursthouse, M. B.; Light, M. E. *Chem.—Asian J* **2010**, *5*, 555−561. (c) Jia, C.; Wu, B.; Li, S.; Yang, Z.; Zhao, Q.; Liang, J.; Li, Q.-S.; Yang, X.-J. *Chem. Commun.* **2010**, *46*, 5376−5378.

(25) Hay, B. P.; Firman, T. K.; Moyer, B. A. *J. Am. Chem. Soc.* **2005**, *127*, 1810−1819.